International Journal of Electrical and Power Engineering 1 (3): 264-273, 2007

Modelling and Control of an Optimized PV Array with Hydrogen System Comprising a PEMFC and an Electrolyzer

[1]Rihab Jallouli, [2]Lotfi Krichen, [2]Bruno Francois and [1]Abderrazak Ouali
[1] Department of Electrical Engineering, National School of Engineering, University of Sfax BP W, 3038, Sfax, Tunisia
[2]Department of Electrical Engineering, Ecole Centrale de Lille, Cite Scientifique, BP48, 59651, Villeneuve d'Ascq, France

Abstract: This research deals with the modelling and the control of a hydrogen system comprising a Proton Exchange Membrane Fuel Cell (PEMFC) and an Electrolyzer (EL) to optimize the power use of a small photovoltaic source. The Photovoltaic panel (PV) provides energy to the load, the excess energy produced, with respect to the load requirements will be sent to the electrolyzer for hydrogen production and storage. Dynamic modelling of various components of this small system is presented. The performances of this source are demonstrated by digital simulation.

Key words: Modelling, fuel cell, electrolyzer, photovoltaic energy, power converters, control

INTRODUCTION

To supply its energy needs, the world relies on fossil fuels. Few years later, it is expected that fossil reserves will not satisfy the growing energy demand. That is why, many researches are leaded to develop new alternative energy sources such as fuel cells, photovoltaic array systems and wind turbine generators (Iqbal, 2003). Production of hydrogen using photovoltaic arrays for later use in a fuel cell seems an efficient alternative to substitute current oils and produce power at a much lower cost and will contribute a much lower amount of CO_2 emission.

The elected fuel cell is a Proton Exchange Membrane Fuel Cell (PEMFC) known by: A low temperature operation; Non pollutant emission: water waste and it uses a polymer solid membrane as an electrolyte, which is easy to construct and to implement (EG and G Services, 2000). However, the mainly concern about fuel cells are their high cost which make research and development a hard task (Vergas *et al*., 2005).

The studied system consists of a PV panel, a PEMFC, an EL and a load. A block diagram of this source is described in Fig. 1. The load can be supplied from the photovoltaic panel or the fuel cell. If the PV panel is producing enough power, the load will be entirely supplied from photovoltaic energy. In study of low solar radiations, the fuel cell will compensate this defect of energy and the power will be supplied from this electrochemical device. If the output power from the PV panel will exceed the demand, the excess power will be sent to the electrolyzer to produce hydrogen from water and to store it in a tank for later use in the fuel cell.

SYSTEM MODELLING

Fuel cell dynamic modelling: Fuel cells are electrochemical devices that convert the chemical energy of a reaction directly into electrical energy. The overall reaction in a fuel cell is represented by:

$$H_2 + \frac{1}{2}O_2 \rightarrow H_2O + \text{Heat} + \text{Electrical energy} \quad (1)$$

The output voltage of a single cell can be defined as the result of the following expression:

$$V_{FC} = E_{Nernst} - V_{act} - V_{Ohm} - V_{Conc} \quad (2)$$

E_{nernst} is the thermodynamic potential of the cell and it represents its reversible voltage; V_{act} is the voltage drop due to the activation of the anode and of the cathode; V_{Ohm} is the ohmic voltage drop and V_{Conc} represents the voltage drop resulting from the concentration or mass transportation of the reacting gases. Each one of the terms in (2) can be calculated using the following expressions (Pudulles *et al*., 2000; Cirrincione *et al*., 2005):

Corresponding Author: Rihab Jallouli, Department of Electrical Engineering, National School of Engineering, University of Sfax BP W, 3038, Sfax, Tunisia

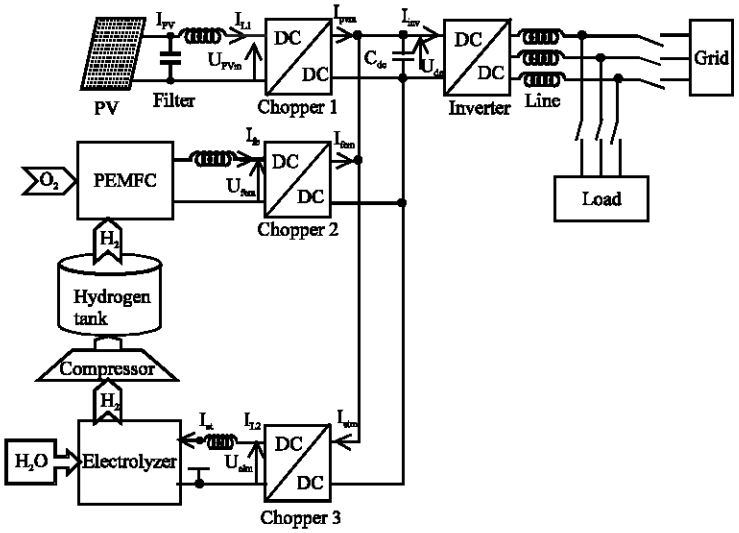

Fig. 1: Propsed photovoltaic/free cell enegry system

Reversible voltage:

$$E_{Nernst} = 1.229 - 0.85\times10^{-3}\times\left(T_{fc} - 298.15\right) + 4.31\times10^{-5}\times T_{fc}\times\left[ln\left(P_{H2}\right) + \frac{1}{2}\times ln\left(P_{O2}\right)\right] \quad (3)$$

Where P_{H2} and P_{O2} are H_2 and O_2 partial pressures respectively and T_{fc} is the fuel cell temperature.

Activation overpotential: The voltage drop due to the activation of the anode and of the cathode is described by:

$$Vact = \begin{bmatrix}\xi_1 + \xi_2.T_{fc} + \xi_3.T_{fc}.\ln(co_2) \\ + \xi_4.T_{fc}.\ln(I_{fc})\end{bmatrix} \quad (4)$$

Where ξ_i are the parametric coefficients based on electrochemical, kinetics and thermodynamics laws, I_{fc} is the fuel cell actual current and co_2 is the oxygen concentration in the catalytic interface of the cathode.

Ohmic overpotential: The ohmic drop is associated with the conduction of the protons through the solid electrolyte and electrons through the internal electronic resistances:

$$V_{Ohm} = I_{fc}\times\left(R_M + R_C\right) \quad (5)$$

Where is the equivalent membrane resistance (Ω) and R_C is the membrane equivalent contact resistance.

Concentration overpotential: The voltage drop resulting from the concentration or mass transportation of the reacting gases can be expressed by:

$$V_{Conc} = -B\times ln\left(1 - \frac{J}{J_{max}}\right) \quad (6)$$

Where B is the parametric coefficient used in the calculation of the concentration losses, J is the actual fuel cell current density and J_{max} is the maximum current density.

The gas concentration can be calculated using the following equation. For oxygen, for example, we have (Padulles *et al*., 2000; Cirrincione *et al*., 2005).

$$co_2 = \frac{P_{O2}}{5.08\times10^6.e^{-(498/T_{fc})}} \quad (7)$$

The equivalent membrane resistance can be calculated by:

$$R_M = \frac{\rho_M\times1}{A_{fc}} \quad (8)$$

Where I is the membrane thickness, A_{fc} is the membrane active area and P_M is the membrane specific resistivity (Ω. cm), which can be obtained by:

$$\rho_M = \frac{181.6\left[1 + 0.03\left(\frac{I_{fc}}{A_{fc}}\right) + 0.062\left(\frac{T_{fc}}{303}\right)^2\left(\frac{I_{fc}}{A_{fc}}\right)^{2.5}\right]}{\left[\psi - 0.643 - 3\left(\frac{I_{fc}}{A_{fc}}\right)\exp\left[4.18\left(\frac{T_{fc} - 303}{T_{fc}}\right)\right]\right]} \quad (9)$$

Charge double layer: To consider the FC dynamics, the phenomenon known as charge double layer should be taking into account. This phenomenon means that there is a first order delay in the dynamic operation of FCs, affecting the activation and the concentration voltages. The differential equation stating this dynamic relationship is represented by Correa *et al.* (2003):

$$\frac{dv_d}{dt} = \frac{1}{C} I_{fc} - \frac{1}{t} v_d \quad (10)$$

Where V_d represents the FC dynamic voltage, C is the equivalent electrical capacitance and τ is the FC electrical time constant defined by:

$$t = C \cdot R_a = C \cdot \left(R_{act} + R_{con}\right) = C \cdot \left(\frac{V_{act} + V_{con}}{I_{fc}}\right) \quad (11)$$

Molar flow rates and pressures: Both hydrogen and oxygen pressures depend on the inlet flow rate of the fuel and the air, considered as the oxidant for the fuel cell. The molar flow rates of hydrogen and air in standard moles per second are expressed as (Davis, 2000):

$$m_{H2} = \frac{P_s \times 1.2}{2 \times F \times V_{FC}} \quad (12)$$

$$m_{O2} = \frac{P_s \times 2.5}{4 \times F \times V_{FC} \times 0.21} \quad (13)$$

Where 0.21 in (13) refers to the ratio of oxygen in air, V_{FC} is the FC voltage (V) obtained from (2) and P_S is the stack electrical power (W), obtained from:

$$P_S = n_c \times V_{FC} \times 1_{fc} \quad (14)$$

and n_c is the number of cells used in the stack.

The gas pressures within fuel cell stack can be determined using the mole conservation principle. For the fuel cell anode we can write (Francois *et al.*, 2005):

$$\frac{dP_{H2}}{dt} = \frac{R}{V_a} T_{fc} \left(m_{H2} - \frac{I_{fc}}{2F}\right) \quad (15)$$

Where m_{H2} is the fuel molar flow rate into the stack compartment, V_a is anode volume in liters, R is universal gas constant, T_{fc} is fuel cell temperature (K) and F is Faraday constant. Similarly, the cathode equation is:

$$\frac{dP_{O2}}{dt} = \frac{R}{V_c} T_{fc} \left(m_{O2} - \frac{I_{fc}}{4F}\right) \quad (16)$$

Where V_c is the cathode volume in liters.

The polarization curve of a fuel cell (Fig. 2) represents its output voltage against the load current or the load current density. This curve shows how the FC voltage behaves when the load current changes (Francios *et al.*, 2005).

Electrolyzer modelling: Most used models of electrolyzers in the current literature are alkaline electrolysers. The electrolyte used in the conventional alkaline water electrolyzers has traditionally been aqueous potassium hydroxide (KOH) (Ulleeberg, 2003). Where the potassium ion and hydroxide K^+ take care of the ionic transport. The typical operating temperatures and pressures of these electrolyzers are 70-100°C and 1-30 bars, respectively. Physically an electrolyzer stack consists of several cells linked in series. The total reaction for splitting water is:

$$H_2O(1) + \text{electrical energy} \rightarrow H_2(g) + \frac{1}{2} O_2(g) \quad (17)$$

An electrolyzer presents several aspects: Electrical, electro-chemical and the thermodynamic one.

Electrical aspect: An electrolyzer cell can be modelled using empirical current-voltage (I-U) relationships. Several empirical models for electrolyzers have been suggested. The basic form of the (I-U) curve used in this study is, for a given temperature:

$$U = U_{rev} + \frac{r_1 + r_2 T_{el}}{A_{el}} I_{el} + \left(s_1 + s_2 T_{el} + s_3 T_{el}^2\right) log\left(\frac{t_1 + t_2/T_{el} + t_3/T_{el}^2}{A_{el}} I_{el} + 1\right) \quad (18)$$

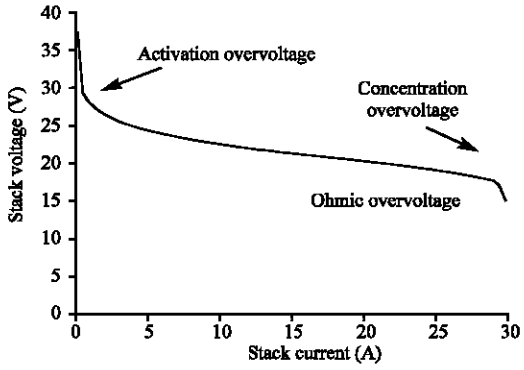

Fig. 2: Polarization curve of the fuel cell

Where U_{rev} is the reversible cell voltage varying slowly with the temperature and pressure, r_i are the parameters for ohmic resistance of electrolyte, s_i and t_i are the parameters for over-voltage on electrodes, A_{el} is the area of the electrode, T_{el} is the temperature of the electrolyte and I_{el} is the electrolyzer current.

Electro-chemical aspect: The total hydrogen production rate in an electrolyzer, which consists of several cells connected in series, can be expressed as:

$$m_{el\_pro} = \eta_F \cdot \frac{n_s \cdot I_{el}}{n \cdot F} \quad (19)$$

Where m_{el_pro} is the hydrogen production rate, η_F is the Faraday efficiency, n_s is the number of cells in series, n is the number of moles of electrons per mole of water (n = 2) and F is the Faraday constant.

The Faraday efficiency η_F is defined as the ratio between the actual and theoretical maximum amount of hydrogen produced in the electrolyzer.

$$\eta_F = a_1 \exp\left(\frac{a_2 + a_3 T_{el} + a_4 T_{el}^2}{I_{el}/A_{el}} + \frac{a_5 + a_6 T_{el} + a_7 T_{el}^2}{(I_{el}/A_{el})^2}\right) \quad (20)$$

Where a_i are adjustable parameters.

Thermo dynamical aspect: According to the ideal gas law, the hydrogen pressure in the electrolyzer P_{el} can be calculated from:

$$p_{el} = \frac{RT_{el}}{V_{el}} n_{el} \quad (21)$$

Where R is the universal gas constant, T_{el} is the electrolyzer temperature considered as constant to simplify the modelling, V_{el} is the cathode volume and N_{el} is the hydrogen quantity stored in the cathode. This quantity can be described as following:

$$n_{el}(t_0 + dt) = n_{el}(t_0) + \int_{t_0}^{t_0+dt} m_{el}(t)\,d(t) \quad (22)$$

$n_{el}(t_o)$ is the hydrogen quantity already existing in the cathode, $m_{el}(\tau)$ is the hydrogen rate evolution through the cathode and it depends on both elements the production rate M_{el_pro} and the outlet rate M_{el_out}:

$$m_{el} = M_{el\_pro}\, M_{el\_out} \quad (23)$$

Compressor modelling: The compressor model is based on polytropic compression process. The compressor work required for this process can be written as:

$$W_{comp} = \frac{kRT_{el}}{k-1}\left[\left(\frac{p_{sto}}{p_{el}}\right)^{\frac{k-1}{k}} - 1\right] \quad (24)$$

Where P_{STO} is the tank hydrogen pressure, P_{el} is the electrolyzer hydrogen pressure and k is the polytropic coefficient assumed equal to 1, 4.

The compressor power is written as:

$$P_{comp} = \frac{W_{comp} m_{el}}{\alpha_{comp}} \quad (25)$$

Where α_{comp} is the compressor efficiency assumed equal to 63% and m_{el} is the hydrogen molar flow inlet the compressor considered equal to that outlet the electrolyzer.

HYDROGEN TANK MODELLING

The quantity of hydrogen outlet the compressor is considered equal to that inlet the tank (we neglect the leakage) so the number of stored moles in the tank is:

$$n_{sto}(t_0 + dt) = n_{sto}(t_0) + \int_{t_0}^{t_0+dt} m_{el\_out}(t)\,d(t) \int_{t_1}^{t_1+dt} m_{fc}(t)\,d(t) \quad (26)$$

Where $m_{el\text{-}out}$ comp is the hydrogen outlet flow rate from the electrolyzer and m_{fc} is the outlet flow rate from the tank to the FC in later time, since the electrolyzer and the fuel cell never work simultaneously.

According to the ideal gas law, the hydrogen tank pressure $p_{sto}$is:

$$p_{sto} = \frac{RT_{sto}}{V_{sto}} n_{sto} \quad (27)$$

Where T_{sto} is the tank temperature considered as constant and V_{sto} is the tank volume assumed equal to 5 litres.

Photovoltaic panel modelling: A photovoltaic panel consists of photovoltaic cells linked in series or in parallel. It is defined by its power in the standard conditions tests,

its voltage and its current (Maouedj, 2006). The photovoltaic panels have been largely studied for more than 20 years. The empirical model, currently used, is the one with a diode. The equivalent electric circuit of the PV model is described by the following equation:

$$I = I_L - I_D - I_{Sh} = I_L - I_0\left[exp\left(\frac{U + IR_S}{a}\right) - 1\right] - \frac{U + IR_S}{R_{Sh}} \quad (28)$$

Where:

I_L : Radiation current (A)
I_O : The diode saturation current (A)
R_S, R_{sh} : Series and shunt resistance (Ω)
α : Fitting parameter of the module (V)
U : The module voltage (V)
I : The module current (A)

POWER ELECTRONICS MODELLING

The modelling of the converters is made by using the concept of instantaneous average value (Francois and Hautier, 1999; Robyns *et al*., 2002) Indeed, this type of modelling is interesting since it adapts well to a numerical integration so it is not necessary to choose a step of integration lower than the period of operation of the converters. Moreover, it makes it possible to simulate the total dynamic behaviour of the system.

Modelling of the inverter: A switching function f_{ij} is defined for each power switch (Bosucayrol *et al*., 2005). It represents the ideal commutation orders and takes the values 1 when the switch is closed (on) and 0 when it is opened (off):

$f_{ij} \in \{0, 1\}$

$$\text{with} \begin{cases} i \in \{1,2,3\} \text{ no. of the leg} \\ j \in \{1,2\} \text{ no. of the switch in the leg} \end{cases}$$

For the three-phase inverter 'inv' of Fig. 1, the modulation functions can be defined from the switching functions:

$$m_{inv} = \begin{bmatrix} m_{inv13} \\ m_{inv23} \end{bmatrix} = \begin{bmatrix} 1 & 0 & -1 \\ 0 & 1 & -1 \end{bmatrix} \begin{bmatrix} f_{11} \\ f_{21} \\ f_{31} \end{bmatrix}_{inv} \quad (30)$$

Modelling of the choppers: As the voltages applied to the different parts of our system (PV, FC and EL) described in Fig. 1 are different from the DC bus voltage, a DC-DC converter is required between the DC bus and each component. Thus, the DC bus constitutes the interface between these components and the inverter.

The chopper 1 placed between the photovoltaic source and the DC bus provides the voltage from the capacitor voltage U_{dc} and the modulated current E_{pvm}:

$$\begin{cases} U_{mpv} = m_{pv} . U_{dc} \\ I_{pvm} = m_{pv} . I_{L1} \end{cases} \quad (31)$$

In the fuel cell case, we can notice that the level of current is correlated with the power one. The model of the fuel cell has a voltage source character, so we can eliminate the capacitor element before the chopper (Fig. 1). Hence the electric quantities are:

$$\begin{cases} U_{fcm} = m_{fc} . U_{dc} \\ I_{fcm} = m_{fc} . I_{fc} \end{cases} \quad (32)$$

The DC bus transmits the power to the electrolyzer through the chopper 3. The modulated voltage and current of the electrolyzer U_{elm} and I_{eln} have the following expressions:

$$\begin{cases} U_{elm} = m_{el} . U_{dc} \\ I_{elm} = m_{el} . I_{L2} \end{cases} \quad (33)$$

SYSTEM CONTROL

The purpose of the control scheme is to extract the maximum amount of solar irradiation from the photovoltaic panel and to transform the maximum excess of power into hydrogen to be stocked in the tank and to be used later, in case of default energy, by the fuel cell.

MPPT control of the PV panel: The PV module generates the dc power, which is transferred to the chopper using MPPT algorithm to optimize the transmitted photovoltaic power and so to increase the system efficiency (Ahmad and Shenawy, 2006). As an illustration, the energetic representation of the PV is depicted in Fig. 3.

Power flow control: The power transmitted to the electrolyzer is correlated with the level of modulated voltage applied to this device. So, a power regulation can be done with a voltage one:

$$m_{ref} = \frac{U_{elm}}{U_{dc}} \quad (34)$$

Electrolyzer pressure control: To control the electrolyzer pressure we need to optimize the hydrogen outlet flow rate. So a comparison between simulated and measured data must be done. A reference pressure level was imposed (P_{el_ref} = 1.5 bar) and according to the ideal gas law, the reference number of moles is:

$$n_{el\_ref} = \frac{V_{el}P_{el\_ref}}{RT_{el}} \tag{35}$$

and the measured number of moles is:

$$n_{el\_mes} = \frac{V_{el}P_{el\_mes}}{RT_{el}} \tag{36}$$

Thus, through a closed loop control with a corrector C_m, the reference hydrogen variation rate is:

$$m_{el\_ref} = C_m\left(n_{el\_ref} - n_{el\_mes}\right) \tag{37}$$

The hydrogen outlet rate depends on the estimated production rate $m_{el\_pro\_mes}$ and the evolution rate through the cathode m_{el_ref}:

$$m_{el\_out\_ref} = m_{el\_pro\_mes} - m_{el\_ref} \tag{38}$$

The quantity mentioned above is obtained from the measured current:

$$m_{el\_pro\_mes} = a_1 \exp\left(\frac{a_2 + a_3T_{el} + a_4T_{el}^2}{I_{mes}/A_{el}} + \frac{a_5 + a_6T_{el} + a_7T_{el}^2}{\left(I_{mes}/A_{el}\right)^2}\right)\cdot\frac{n_s \cdot I_{el}}{n \cdot F} \tag{39}$$

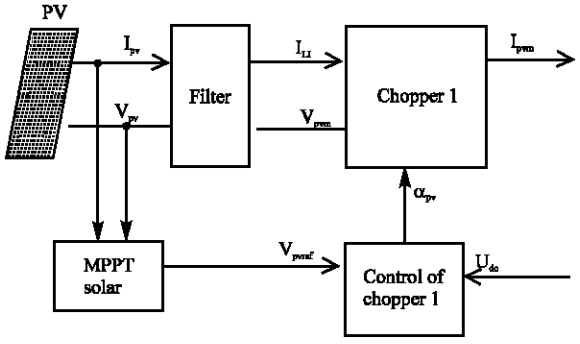

Fig. 3: Energetic represention of the PV

Hydrogen flow control: There are several possibilities for storing hydrogen; the chosen method is to compress the fuel. An electrolyzer can be pressurized at high pressures, while higher pressures in the storage tank require additional hydrogen compression. These compressors require electricity. The selected pressure in the storage tank in this study was 11 bars. The compressor must transfer the gas to the hydrogen tank at the imposed reference outlet flow rate $m_{el\_out\_ref}$. So, the real compressor work is obtained by:

$$P_{comp} = \frac{W_{comp\_mes}}{\alpha_{comp}} m_{el\_out\_ref} \tag{40}$$

The estimated polytropic work W_{comp_mes} is:

$$W_{comp\_mes} = \frac{kRT_{el}}{k-1}\left[\left(\frac{p_{sto\_mes}}{p_{el\_mes}}\right)^{\frac{k-1}{k}} - 1\right] \tag{41}$$

The continuous bus control: The DC bus is the central element of the whole production system and plays the role of the interface between the various components. This DC bus voltage is governed by the following differential equation:

$$C_{dc}\frac{dU}{dt} = I_{rem} - I_{inv} \tag{42}$$

Where: C_{dc} represents the capacitance of the DC bus and I_{rem} is the total current of the whole system as shown in Fig. 4.

The PV source and the hydrogen system are connected to the DC bus and then to the load or to the system power via the inverter and a line (Fig. 5). This converter makes it possible to control the continuous voltage and the active and reactive powers exchanged with the grid and to establish the currents at the adequate frequency $\omega_s = 100\pi$ rad. s^{-1}.

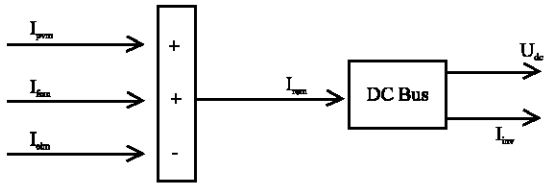

Fig. 4: Energetic represention of the DC bus

In order to generate and send a current to the grid/load, the DC bus voltage 'U_{dc}' has to be higher than the peak value of the voltage (phase to phase) appearing on the side of the filter.

So

$$U_{dc} > \sqrt{6}.V_{rms}$$

where V_{rms} is the rms value of the simple voltage appearing side of the filter. Since $V_{rme} = 127V$, we have imposed $U_{ref} = 400V$. The control block permits the regulation of the DC voltage and the control of the reactive power and so the control of the inverter. We have chosen the unity power factor strategy i.e. the reactive power is set to zero ($Q_{ref} = 0$) with sinusoidal absorption. From the voltage reference U_{ref} and taking into account of the DC bus power and the copper losses in the line, we obtain the active power reference P_{ref}.

The reference powers give the d- and q-axis reference currents Ii_{dref} and I_{iqref} (Krichen, 2007).

Global control of the studied source: The global control of the studied source is independent of the power structure. This strategy leads to achieve power objectives and system constraints and constitutes the power control loop. The electrolyser is powered as long as the available renewable power is greater than the electric load demand. When the hydrogen storage tank is full, the electrolyser is not powered. The excessive power that could be produced in this event is transmitted to the power system. The fuel cell is operated when there is a requirement for power, and hydrogen is available from storage. The supervising system controls the overall current flow

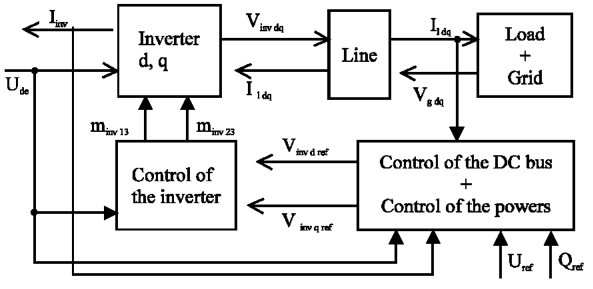

Fig. 5: Energetic represention of the load/grid part

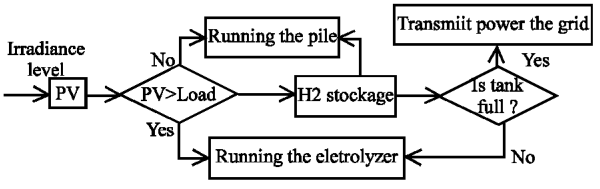

Fig. 6: Flow chart of the global control state

taking into account of the power supplied by the PV panel, the energy demands of the load and the hydrogen system following the flow chart of Fig. 6.

RESULTS

The model of this system has been simulated using the parameters in (Ulleberg, 2003; Correa *et al*., 2003). The irradiation level used in the simulation process, depicted in Fig. 7, is given for 3 typical days (March 14-16th 2005). The load power is represented in Fig. 8. The evolution of fuel cell power and electrolyzer one show the operation range of each device and depend on the load power demand and photovoltaic panel power; these powers are given in Fig. 9 and 10, respectively.

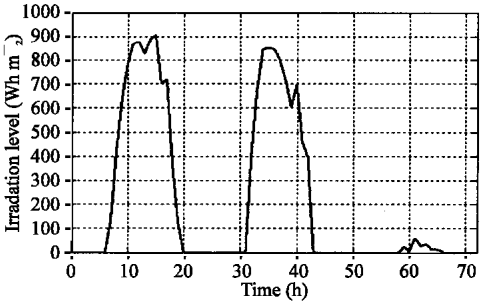

Fig. 7: Irradiance level

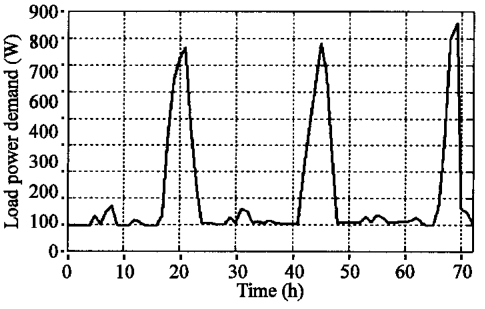

Fig. 8: Load power demand

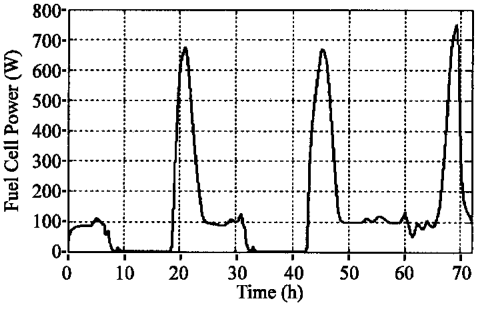

Fig. 9: PEMFC power

The dynamic behaviour of a cell stack of 32 series connected has been simulated. The cell has been fed with hydrogen as fuel and oxygen as oxidant. Starting from a given load power. Figure 9, 11 and 13 show the obtained waveforms of the cell stack power, current and voltage, respectively. These figures show clearly that when the power demand exceed the photovoltaic panel power the fuel cell start running, an increasing in the load current entrain a reduction of the stack voltage with an increase of the generated power. When the power demand is less than the PV panel one, the FC stop running and the excess current is used by the electrolyzer to transform the electrical energy into chemical one to produce hydrogen. Figure 10, 12 and 14 show the obtained waveforms of the electrolyzer power, current and voltage, respectively.

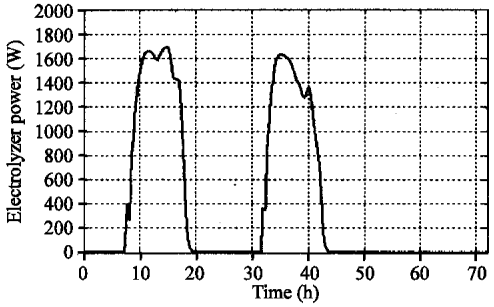

Fig. 10: Electrolyzer power

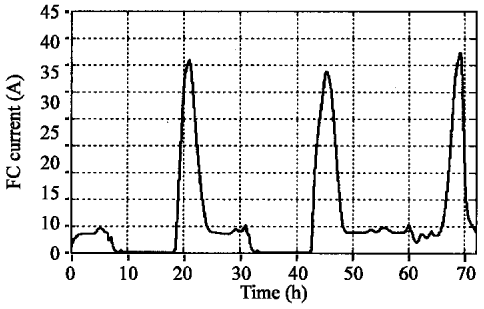

Fig. 11: PEMFC current

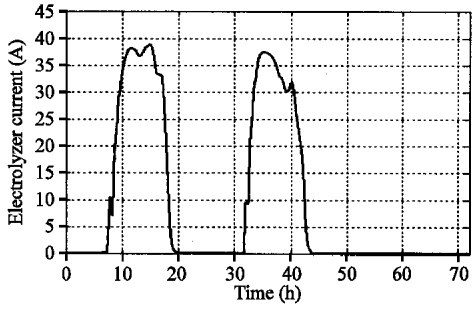

Fig. 12: Electrolyzer current

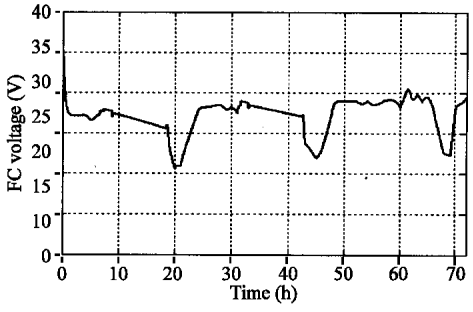

Fig. 13: PEMFC voltage

The conversion function m_{fc} of the chopper 2 and the modulated current associated to the fuel cell, shown in Fig. 15 and 17, depend on the fuel cell voltage and current, respectively. In the same way, the conversion function m_{el} of the chopper 3 and the modulated current associated to the electrolyzer, shown in Fig. 16 and 18, depend on the electrolyzer voltage and current, respectively.

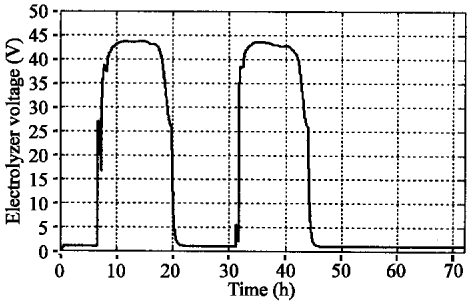

Fig. 14: Electrolyzer voltage

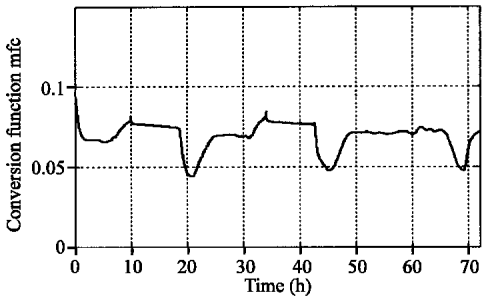

Fig. 15: PEMFC conversion function

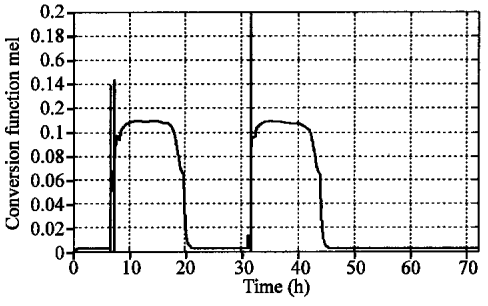

Fig. 16: Electrolyzer conversion function

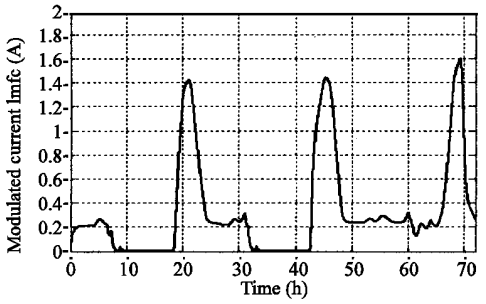

Fig.17: Modulated current of the PEMFC

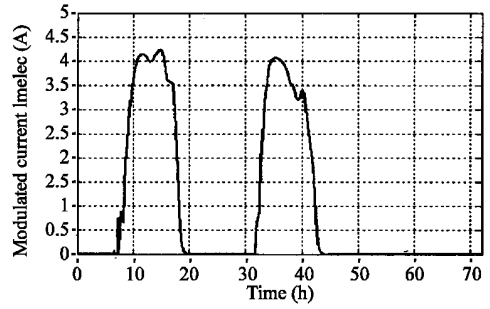

Fig. 18: Modulated current of the electrolyzer

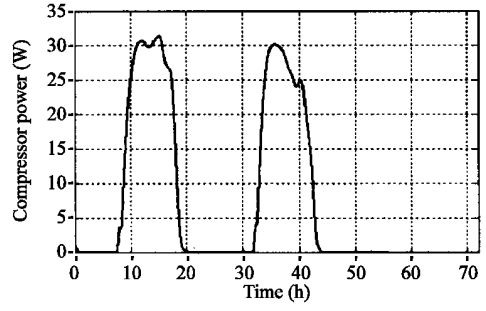

Fig. 19: Compressor power

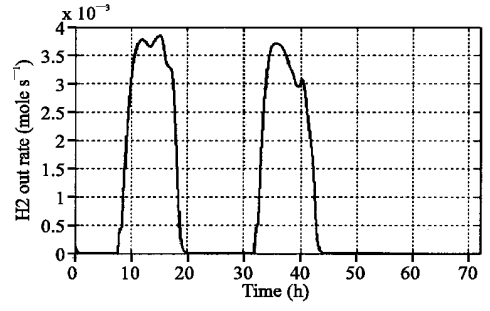

Fig. 20: H2 out rate

The compressor powerP_{comp}, depicted in Fig. 19, contributes to regulate the outlet hydrogen flow rate, which is represented in Fig. 20 for a certain pressure chosen as a reference. Figure 21 shows that the hydrogen

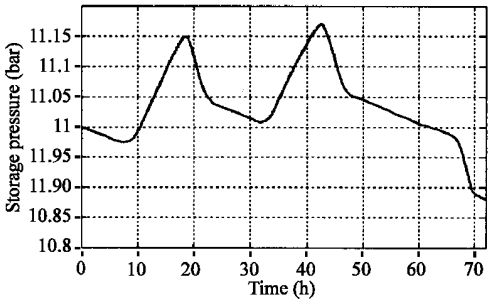

Fig. 21: Storage pressure

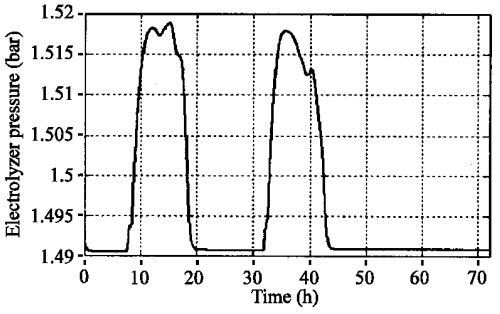

Fig. 22: Electrolyzer pressure

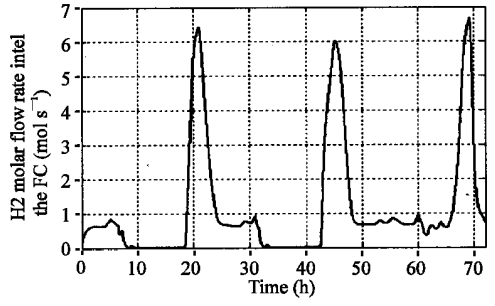

Fig. 23: H2 molar flow rate inlet the FC

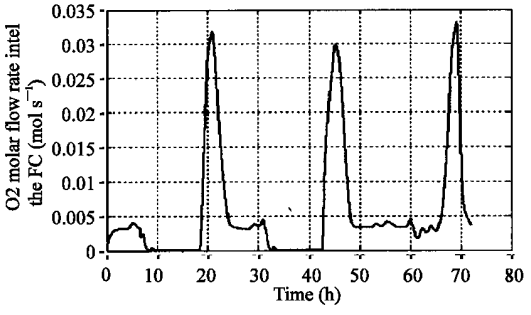

Fig. 24: O2 molar flow rate inlet the FC

pressure in the tank P_{sto} depends on the number of moles stored in the tank n_{el_out}(Fig. 20), also it depends on the molar outlet the tank to the fuel cell (Fig. 23). The oxygen molar flow rate inlet the fuel cell, correlated to its current, is depicted in Fig. 24.

CONCLUSION

A small photovoltaic fuel cell hybrid energy system is proposed in this study. The system modelling, simulation and the controller design are presented. The simulation results show the expected transients in the system during some possible situations. After any change in the radiation level or in the load power, each device in the system reacts in such way to compensate the missing power and to satisfy the load demand.

REFERENCES

Ahmad, G.E. and E.T. El-Shenawy, 2006. Optimized photovoltaic system for hydrogen production. Renewable Energy, pp: 1043-1054.

Bouscayrol, A., P.H. Delarue and X. Guillaud, 2005. Power strategies for maximum control structure of a wind energy conversion system with a synchronous machine. Renewable Energy, 30: 2273-2288.

Cirrincione, M., M. Pucci, G. Cirrincione and M. G. Simões, 2005. A Neural Non-linear Predictive Control for PEM-FC. J. Elec. Sys., 1-2, pp: 1-18.

Corrêa, J.M., F.A. Farret, J.R. Gomes and M.G. Simões, 2003. Simulation of Fuel-Cell Stacks Using a Computer-Controlled Power Rectifier With the Purposes of Actual High-Power Injection Applications. IEEE Trans. Ind. Appiled Vol. 39.

Corrêa, J.M., F.A. Farret, J.R. Gomes and M.G. Simões, 2003. Simulation of fuel cell stacks using a computer controlled power rectifier with the purposes of actual high power injection applications," IEEE. Trans. Ind. Applied, 4: 1136-1142.

Davis, M.W., 2000. Development and Evaluation of Test Apparatus for Fuel Cells. Masters Thesis, Virginia Polytechnic Institute State University, Virginia.

EG and G Services, 2000. Fuel Cell Handbook. (5th Edn.), Parsons Inc., DEO of Fossil Energy, National Energy Technology Laboratry.

François, B. and J.P. Hautier, 1999. Commande d'un onduleur triphasé de tension par modulateur de largeur et de position d'impulsions. Revue Internationale de Génie Electrique, 2: 359-387.

Iqbal, M.T., 2003. Simulation of a small wind fuel cell hybrid energy system. Renew. Energy, 28: 511-522.

Krichen, L., 2007. Modeling and control of a hybrid renewable energy production unit. Accepted in Automatic Control and Scientific Engineering (ACSE).

Maouedj, R., A. Deliou and B. Benyoucef, 2006. Modélisation et simulation des performances d'une cellule photovoltaïque. CERE, Hammamet, Tunisia, pp: 06-08CD ROM.

Padullés, J., G.W. Ault and J.R. McDonald, 2000. An integrated SOFC plant dynamic model for power systems simulation. J. Power Sources, 86: 495-500.

Robyns, B., Y. Pankow, L. Leclercq and B. François, 2002. Equivalent continuous dynamic model of renewable energy systems. Seventh International Conference on Modelling and Simulation of Electric machines, Converters and Systems: Electrimacs CD, Aout, Montreal, Canada, pp: 18-21

Ulleberg, O., 2003. Modelling of advanced alkaline electrolyzers: A system simulation approach. Int. J. Hydrogen Energy, 28: 21-33.

Vergas, J.V.C., J.C. Ordonez and A. Bejan, 2005. Constructal PEM fuel cell stack design. Int. J. Heat Mass Transfer, pp: 4410-4427.